Numerical Modelling of an Axial-Field Solid Disk Induction Machine

Marco Angeli
Istituto di Energetica, Università di Perugia, St. S. Lucia Canetola, 06125 Perugia

Nunzio Esposito, Antonino Musolino, Bernardo Tellini
Dipartimento di Sistemi Elettrici e Automazione, Università di Pisa, via Diotisalvi 2, 56126 Pisa

***Abstract*—In this paper a method for the steady-state analysis of an axial-field induction motor with a solid disk rotor is proposed. The boundary condition for the axial component of the magnetic flux density has been calculated by means of an analytical procedure. Accordingly the simulation region is restricted to the air-gap and the rotor. Then the axial component of the diffusion equation is solved for by using a finite difference scheme. Subsequently the azimuthal component of the magnetic flux density and the current density induced in the rotor come out from the field's laws. The validity of the proposed method has been tested by comparing the numerical results with data measured on a double-stator prototype. Finally the numerical procedure has been used for the analysis of the performance of a motor for light vehicle propulsion and the results of the simulation are shown.**

I. Introduction

A lot of research work has been carried out in the past on axial-field induction machines. The magnetic field analysis of these kinds of asynchronous machines gives detailed information about the electromagnetic and the mechanical quantities. This is particularly useful for design and control purposes, these machines being especially promising for vehicle propulsion [1].

Numerical methods are powerful but they require a large amount of memory and CPU time because of the movement of the rotor with respect to the stator. Therefore some attempt to analytically analyse the steady-state behaviour of the axial-field induction motors has been made. In particular an analytical method was presented in a previous paper [2]. In that paper the axial dependence of the variables was neglected but the results were interesting and encouraging. Therefore we have continued the work and we have developed an analytical-numerical procedure that restricts the simulation region to the air-gap and the rotor, reducing the computational effort.

II. Description of the Procedure

A developed view of the structure of an axial-field induction machine is shown in Fig. 1. The two stator cores and the conductive rotor are in the shape of disks. The quasi-stationary magnetic form of the Maxwell's equations is well-suited to the problem. Moreover we consider the conductivity of the rotor as uniform constant. Owing to the harmonic behaviour of the source and the steady-state operating condition considered, phasor notation (in bold) is utilised. Taking account of the movement and combining Ohm's, Ampere's and Faraday-Neumann's laws we obtain the following equations for the magnetic flux density in the air-gaps and in the conductive rotor:

$$\nabla^2\vec{\mathbf{B}} = 0, \tag{1a}$$

$$\nabla^2\vec{\mathbf{B}} = \mu_0\sigma\left(j\omega\vec{\mathbf{B}} - \nabla\times\left(\vec{\omega}_r\times\vec{r}\times\vec{\mathbf{B}}\right)\right). \tag{1b}$$

where σ is the rotor conductivity, ω is the pulsation of the source and ω_r is the angular speed of the rotor. We have solved (1) in the cylindrical region enclosing the air-gap and half of the rotor. The simulation region is shown in Fig. 1.

A. Analytical Calculation of the Boundary Condition

As the first step, the value of the axial component of the magnetic flux density $\mathbf{B}_z$ on the surfaces S_b and S_c of the simulation region is determined by means of the analytical method proposed in [2]. On the end surface S_a a symmetry condition is used. The analytical method provides that the stator windings are modelled on the stator air-gap interfaces as a current sheet having radial and azimuthal components which are dependent on r and φ coordinates. The following simplifying hyphothesis were also provided for by the analytical method. The fields have a sinusoidal profile in the azimuthal direction. The magnetic flux density in the air-gap

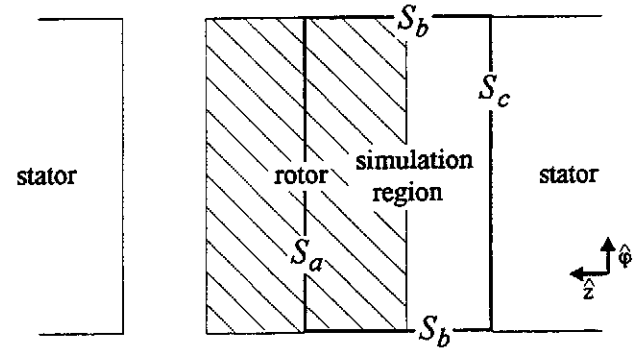

Fig. 1. Basic components of a double-stator axial-field machine; bold line bounds the simulation region.

Manuscript received September 23, 1996.

Marco Angeli, e-mail angeli@turbo.isten.ing.unipg.it, fax + 39 75 585 2703; Nunzio Esposito, e-mail esposito@dsea.unipi.it, fax + 39 50 565 333; Antonino Musolino, e-mail musolino@dsea.unipi.it; Bernardo Tellini, e-mail bernardo.tellini@dsea.unipi.it.

and in the rotor volume is assumed to be axially directed due to the presence of the stator core. This condition is practically verified in actual machine for commonly adopted stator to rotor radius ratios. Moreover the current density induced in the rotor is assumed to be independent of the axial coordinate because the magnitude of the rotor thickness is less than the skin depth under any operating condition. With these assumptions we obtain the following expression for the phasor $\mathbf{B}_z$:

$$\mathbf{B}_z = \frac{-1}{j\omega\sigma s}\left(jp\frac{\mathbf{G}_r}{r} + \frac{\mathbf{G}_\varphi}{r} + \frac{d\mathbf{G}_\varphi}{dr} \right). \tag{2}$$

where s is the slip and p is the number of pole-pairs. $\mathbf{G}_r(r,\varphi)$ and $\mathbf{G}_\varphi(r,\varphi)$ are the phasors related to the radial and the azimuthal component of the rotor current density. The magnetic flux and the rotor current densities have been connected to the stator current sheet by means of the integral form of the Ampere's law. The surfaces S_r and S_φ, shown in Fig. 2a) and 2b) respectively, have been considered for the flux determination. The expressions obtained are:

$$-\frac{jph}{\mu_0 r}\mathbf{B}_z = \mathbf{I}_r + \delta\mathbf{G}_r, \tag{3}$$

$$-\frac{h}{\mu_0}\frac{d\mathbf{B}_z}{dr} = \mathbf{I}_\varphi + \delta\mathbf{G}_\varphi. \tag{4}$$

where $\mathbf{I}_r$ and $\mathbf{I}_\varphi$ are the phasors related to the expression of the stator current density. h is the distance between the stators and δ is the rotor thickness. Following the analytical method proposed in [2], combining (2), (3) and (4) two differential equations for the radial and azimuthal component of the rotor current density are obtained. If the hyphothesis of thin rotor holds, i.e., it can be assumed that $hp^2/\omega\mu_0\sigma s >> \delta r^2$, $\mathbf{G}_r$ is easily determined as:

$$\mathbf{G}_r = \frac{\omega\mu_0\sigma s r^2}{jhp^2 - \omega\mu_0\sigma s\delta r^2}\mathbf{I}_r. \tag{5}$$

Substituting (5) in (2) the expression for the axial component of the magnetic flux density is obtained:

$$\mathbf{B}_z = \frac{-p\mu_0 r}{jhp^2 - \omega\mu_0\sigma s\delta r^2}\mathbf{I}_r. \tag{6}$$

Expression (6) has been used in order to determine the value of the axial component of the magnetic flux density on the surfaces S_b and S_c of the simulation region. On the end surface S_c the value of the boundary condition depends on the radial coordinate; moreover it has a sinusoidal profile in the azimuthal direction.

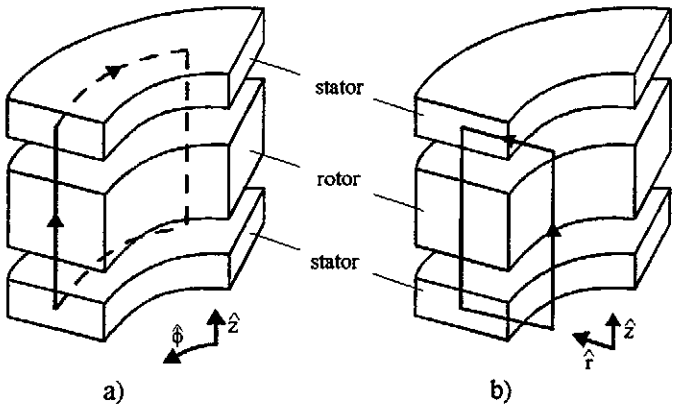

Fig. 2. Closed paths used to express the flux of the Ampere's law:
a) flux through the area S_r;
b) flux through the area S_φ.

B. Numerical Solution

The second step is the calculation of the magnetic flux density in the simulation region. Only the axial component of the boundary condition has been determined. Therefore the axial component of (1a) and (1b), that is

$$\nabla^2\mathbf{B}_z = 0, \tag{7a}$$

$$\nabla^2\mathbf{B}_z = \mu_0\sigma\left(j\omega\mathbf{B}_z + \omega_r\frac{\partial\mathbf{B}_z}{\partial\varphi} \right), \tag{7b}$$

has been solved apart from the other two components of (1) by means of a three-dimensional finite difference scheme. Then the azimuthal component of the magnetic flux density $\mathbf{B}_\varphi$ has been determined by the solenoidal property of the field and neglecting the radial component $\mathbf{B}_r$, as occurs in the actual axial-field machine:

$$\mathbf{B}_\varphi = -r\int\frac{\partial\mathbf{B}_z}{\partial z}d\varphi. \tag{8}$$

Finally the current density induced in the rotor has been calculated by means of the Ampere's law:

$$\mathbf{G} = \frac{1}{\mu_0}\nabla\times\mathbf{B}. \tag{9}$$

III. Validation of the Procedure

The accuracy of the proposed procedure has been investigated by comparing the numerical results with data measured on an existing double-stator three-phase induction prototype built in the Laboratory of the Electrical System Department of the University of Pisa [3]. The main parameters of this induction machine are summarized in Table I.

TABLE I
Parameters of the Induction Machine used for the Validation Test

Parameter	Symbol	Value
inner stator diameter	D1	280 mm
outer stator diameter	D2	600 mm
total stator core thickness (tooth + yoke)	H	60 mm
internal radius of the disk rotor	R_{in}	90 mm
external radius of the disk rotor	R_{ex}	330 mm
rotor thickness	δ	5 mm
air gap between rotor and stator		4 mm
rotor weight		4.7 Kg
distance between the stators	h	13 mm
number of slots	q	54
chord factor	kp	9/13.5
number of conductors per slot	z	48
number of pole-pairs	p	2

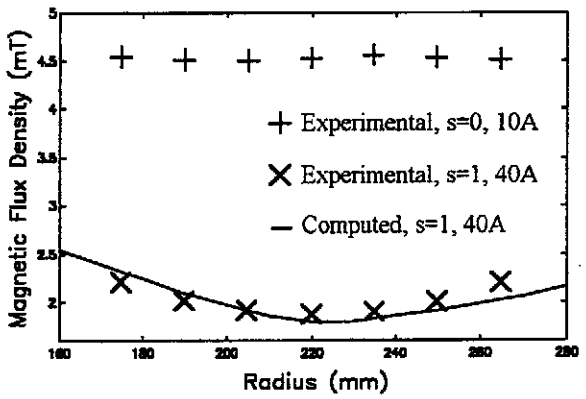

Fig. 3. Amplitude of the magnetic flux density in the air gap between rotor and stator vs. the radial coordinate.

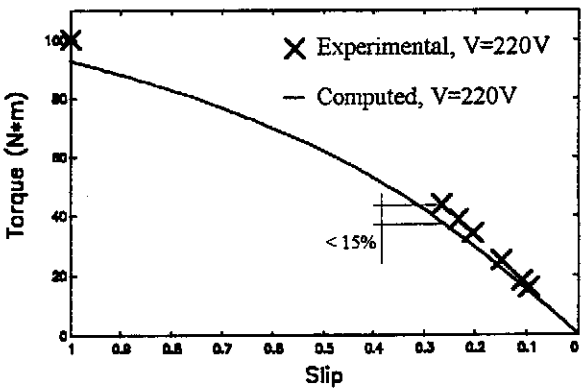

Fig. 4. Comparison between the computed and the experimental mechanical characteristic of the machine.

Some experimental tests on the machine fed by the 50 Hz power network were carried out. These measurements have been used as a benchmark for the validation of the procedure developed.

In Fig. 3 the plus signs represent the amplitude of the magnetic flux density in the air gap measured without the rotor and feeding the stator windings by 10 A current. These data have been used to adjust the intensity of the current sheet modelling the stator windings. Then the magnetic flux density has been calculated setting the slip to 1 and the intensity of the current sheet corresponding to 40 A stator current, as in the experimental test. The increase of the electrical resistivity of the aluminium rotor due to Joule heating has been taken into account by means of the measured temperature. The results obtained by the analytical-numerical procedure are reported in Fig. 3. In the same figure the values measured on the machine are shown by the cross signs.

The mechanical torque has been computed by using the values of the magnetic flux density and the current density induced in the rotor calculated by means of the procedure proposed. The predicted mechanical characteristic has been compared with the experimental data. The comparison shows that the relative error is less than 15%, as can be seen in Fig. 4. This can be considered a good result from an engineering point of view.

In addition we have simulated the behaviour of the motor described in Table I by using the analytical procedure presented in [2]. In this case the values of the torque and the current resulted lower than the ones calculated by means of the procedure here proposed, therefore with a lower accuracy than the present results if compared with respect to measured values.

IV. APPLICATIONS

We have carried out some simulations in order to analyse the performance of a disk induction motor for light vehicle propulsion, fed by a suitable current drive, whose main design parameters are summarized in Table II.

TABLE II
Parameters of the Induction Motor for Light Vehicles Propulsion

Parameter	Symbol	Value
internal radius of the disk rotor	R_{in}	0.03(m)
external radius of the disk rotor	R_{ex}	0.2(m)
rotor thickness	δ	0.01(m)
distance between the stators	h	0.012(m)
rpm range of the drive-shaft	n	0÷600(rpm)

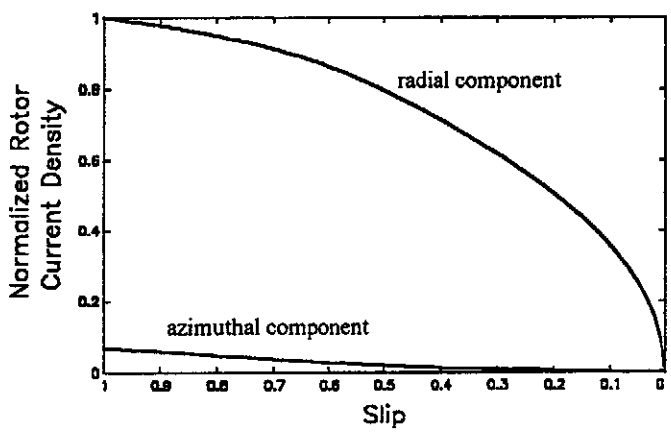

Fig. 5. Normalized components of the rotor current density at f=24Hz and p=2.

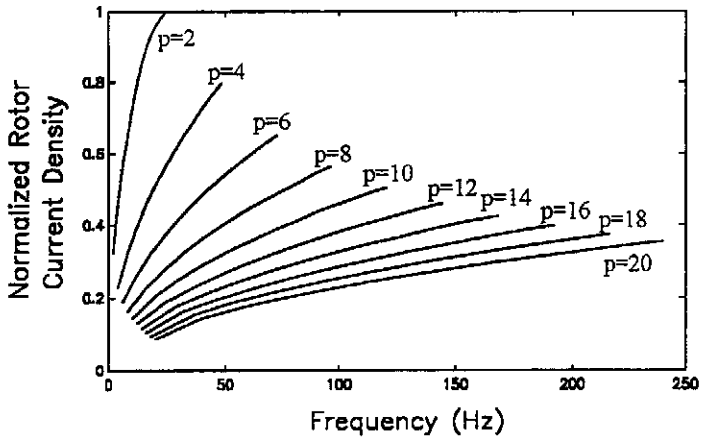

Fig. 6. Rotor current density calculated at s=1 for different pole-pairs number.

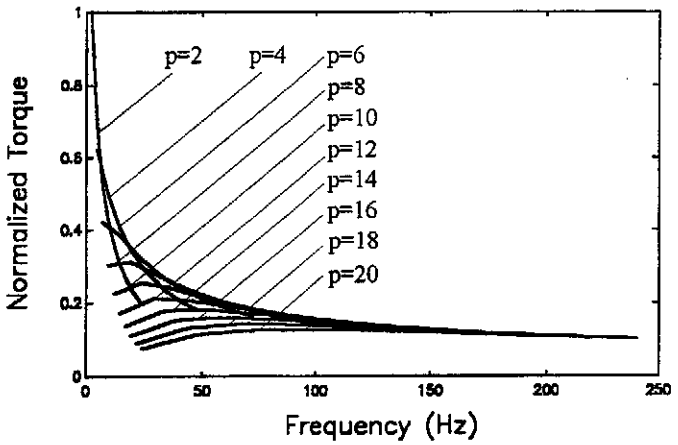

Fig. 7. Normalized torque calculated at s=1 for different pole-pairs number.

Fig. 5 shows the azimuthal and the radial components of the rotor current density as a function of the slip. The values have been calculated at f=24Hz and p=2 and they have been normalized with respect to the maximum value. As known, the current induced stresses the material particularly at the takeoff. On the other hand this is a frequent operating condition in vehicle propulsion.

Then the influence of the number of pole-pairs and the frequency of the power supply on the maximum value of the rotor current has been investigated. For each number of pole-pairs considered we have settled a range of frequency in which the power supply can operate. The upper limit of each range of frequency is equal to $12p$ so that the maximum synchronous speed is fixed to 720 rpm for any number of pole-pairs. As known, a reduction of the current density induced in the rotor at the takeoff is gained by increasing the number of pole-pairs. However the reduction is tangible moving from a low number of pole-pairs and then it becomes quite of no use as the number increases. Such a behaviour can be observed in Fig. 6, where the current density has been normalized with respect to the maximum value. Moreover the frequency of the power supply greatly affects the value of the current density especially at low number of pole-pairs. However as the maximum current density is reduced, the torque at the takeoff is reduced as well, as the data reported in Fig. 7 show. Then a proper choice of the number of pole-pairs will take account of both the safe operating conditions and the required torque at the takeoff. On the contrary, a further increasing of the number of pole-pairs beyond the required value can be useful in order to achieve a quite constant behaviour of the torque vs. the frequency of the power supply at the takeoff.

In Fig. 8 the maximum torque attainable in the range of revolution per minute considered for the drive-shaft is reported. The maximum value is achievable at a well-defined frequency of the power supply. This information is reported in Fig. 9 for different values of the number of pole-pairs and it is useful in order to drive the motor under a maximum torque condition at every speed by varying the frequency of the feed system. It can be noticed that the relationship frequency vs. revolution per minute is quite linear for the lower numbers of pole-pairs; the saturation like effect shown for the higher numbers of pole-pairs is due to the limit settled for the frequency range.

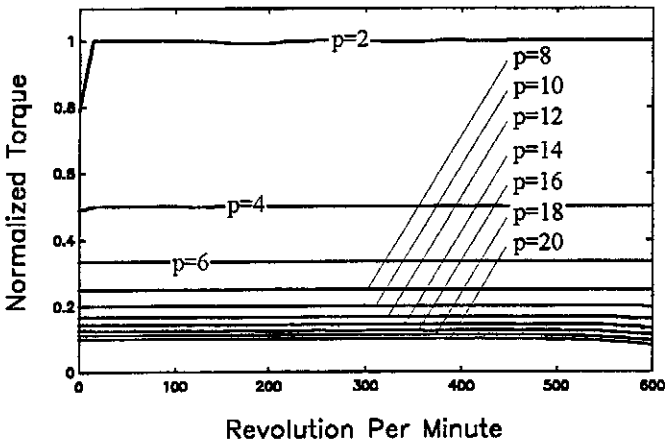

Fig. 8. Maximum torque attainable in the given frequency range for different number of pole-pairs.

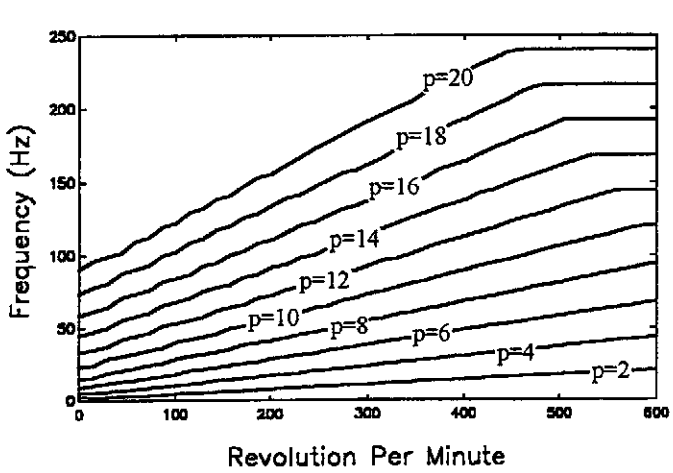

Fig. 9. Frequency of the power supply giving the maximum value of the torque.

V. Conclusions

In this paper we have presented a procedure for the analysis of the steady-state behaviour of axial-field solid disk induction machines. The analytical evaluation of the boundary condition for the axial component of the magnetic flux density has given proof of a negligible loss of accuracy, as the comparison with data measured on a double-stator three-phase induction prototype motor shows.

The analytical-numerical procedure developed can be usefully utilized as a design tool. The model has been used to point out the influence of some design parameters on the electromagnetic and the mechanical performance of these kinds of machines. For instance any choice of the number of pole-pairs provides for benefits on some quantities and for drawbacks on some others.

The procedure appears particularly promising owing to its reduced computational cost with respect to a classical numerical procedure that account for "infinite" boundary. The numerical simulations can be carried out even by a personal computer. As a further development the enhancement of data at our disposal will be performed in order to synthesize the numerical information obtained into compact formula. In this way the optimization of a settled performance index with respect to given design parameters and for a given application will be supported.

References

[1] D. Platt, B. H. Smith, "Twin Rotor Drive for an Electric Vehicle," *IEE Proc.-B*, vol. 140, No. 2, March 1993.

[2] N. Esposito, A. Musolino, B. Tellini, "Electromagnetic Analysis of an Induction Motor with Massive Disk," *IEEE Transaction on Magnetics*, vol. 31, no. 3, 2076-2079, May 1995.

[3] A. Bramanti, R. Dalmazzo, G. Gallanti, A. Tellini, "Experimental research on a prototype of a three-phase induction motor with axial air gap," *Proc. Inter. Conf. on Electrical Machines*, part 1, pp. sp2/2-1-sp2/2-10, Brussels (B), September 11-13, 1978.